Development and verification of a laser profilometer for microtexture assessment of pavement surfaces

G. Baimukhametov
University of Sunshine Coast

G. White
University of Sunshine Coast

S. Jamieson
University of Sunshine Coast

ABSTRACT: Surface friction is one of the most important aspects of safety for runway pavements. Consequently, accurate friction assessment can inform safe aircraft operations. One of the ways to increase the accuracy of friction assessment is to use texture tests. The aim of this study is to develop and verify a simple profilometer and profile picture processing algorithm for microtexture assessment. Such parameters as smothering coefficient and angle between laser and camera and surface were optimized. Laser profilometer testing results correlate well with the stylus-based roughness tester (R^2 = 0.99). The proposed assessment technique can be used for the microtexture assessment during runway friction surveys.

1 INTRODUCTION

1.1 *Surface friction*

Surface friction is one of the most important parameters of pavement affecting runway safety. The friction between a tire and a pavement directly affects the braking performance and maneuverability of aircraft. The coefficient of friction is a complex value that mostly depends on the hysteresis and adhesion effect between two surfaces. Adhesion, however, has a smaller influence on the friction due to the presence of moisture, dust, and other contaminants. Hysteresis effect, due to its nature, mostly depends on surface texture (Ueckerman et al., 2015). Additionally, surface texture lowers the risk of contact loss (hydroplaning) by providing contact patch drainage and reducing the water film thickness on a pavement surface (White, 2024).

Surface friction is generally measured by continuous friction measuring equipment (CFME) (AAA, 2017). However, due to the complexity of the friction phenomena, direct friction measurements by imitating the contact between a tire and a surface usually have low accuracy and repeatability. Changes in humidity, surface temperature, wear of the sliders and tires of the CFME, and the influence of speed make the reliability of the friction measurements poor, which could lead to serious friction-related accidents (Dardano & Wickham, 2005). Consequently, one of the ways to improve the friction management of runways is to add microtexture measurement to the tools for conducting friction surveys on runway pavement surfaces.

1.2 *Surface texture and friction*

Surface texture is a set of surface irregularities. Texture is usually divided into four classes depending on the wavelength; microtexture (up to 0.5 mm), macrotexture (0.5 to 50 mm), megatexture (50 mm to 500 mm), and unevenness (greater than 500 mm). However, only macrotexture and microtexture are important for the braking performance and maneuverability of aircraft. Megatexture and unevenness are usually eliminated due to noise and vibration during aircraft movement (Chen et al., 2022).

Microtexture and macrotexture affect the friction differently at different speed. At high speed, macrotexture lowers the risk of dynamic hydroplaning by improving water drainage. Microtexture, on the other hand, provides good friction at lower speed, by reducing the thickness of the water film and increasing the hysteresis effect (Xiao et al., 2024).

Theoretical and empirical models are used for the friction prediction based on a surface texture (Li et al., 2020). Some of the studies use artificial neural networks to predict surface friction with high accuracy (Yang et al., 2018). Some of the models were used during the development of the International Friction Index system (Wambold et al., 1995).

1.3 *Surface texture measurements*

Macrotexture measurements are usually simple due to the larger size of the surface irregularities. Different methods are standard for macrotexture measurements, such as profilometry and volumetric methods, which are widely used in engineering practice (White et al., 2021). Microtexture testing, however, is more challenging, and in current practice, there is no widely accepted method of microtexture assessment.

In research practice, different methods of microtexture assessment can be used, which can be divided into contact and non-contact methods. Contact methods include such methods as the mechanical stylus test and different wear tests. Non-contact methods are used more often and include laser profilometry, image texture analysis, stereoscopy, computed tomography scanning, 3D scanning, and simpler microscopy assessment methods, such as the straightedge shadow method (Chen et al., 2022).

The most precise and simple method is laser profilometry, which is based on the geometrical measurement of a projection of the laser beam on a surface (Martín-Béjar et al., 2023). However, there is no standard laser profilometer equipment for pavement testing.

The aim of this study is to introduce the design of a cheap and simple laser profilometer for pavement testing, including a profile picture analysis algorithm, and to verify it.

2 MATERIALS AND METHODS

2.1 *Testing surfaces*

To avoid the macrotexture influence, the verification was performed in the laboratory using different samples, including polished metal plates, sandpaper, and a mill file. A total of eight tests were performed by assessing an average roughness (Ra) of the surface, which can be found as an average deviation of the profile point coordinate.

2.2 *Profilometer verification*

Reference surface texture measurements were performed using the Intra Touch roughness tester with 4 nm vertical and 0.5 µm horizontal resolution. This roughness tester is based on the stylus test and provides a precise microtexture measurement. However, the vertical range of that tester allows use only with plain surfaces.

2.3 *Laser profilometer*

A laser profilometer was designed using widely accessible and economically available components (Fig. 1). The total price of profilometer components, excluding the price of the mount, which is made of 3 mm metal sheet, was equal to 36 AUD (24 USD).

The measurement process includes the following steps: positioning of the device on a surface, instantaneous registration of a singular 4 mm long profile, and repositioning the device.

The resolution of the camera was equal to 6.09 µm. Vertical resolution can vary by changing the angle between the camera and a laser. The profilometer mount allows a change in the angle between the laser, camera and surface. The resulting profile is registered as a picture, allowing analysis in the VBA application for Excel.

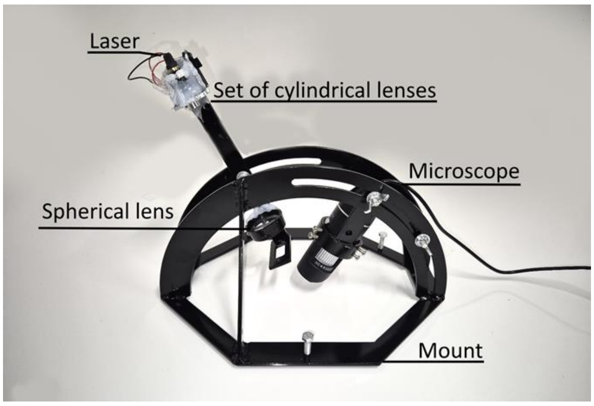

Figure 1. Laser profilometer model

3 RESULTS AND DISCUSSION

3.1 *Profilometer design*

A laser profilometer consists of two main parts; a camera or sensor, and a laser. Depending on the construction of a profilometer, a laser requires a set of lenses to project the laser line on a surface. The profilometer scheme is shown in Figure 2.

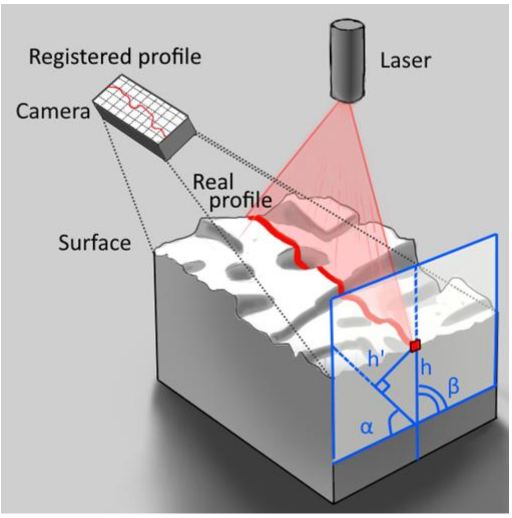

Figure 2. Laser profilometer scheme

The relative height of the profile point on surface and, on registered profile in **Fehler! Verweisquelle konnte nicht gefunden werden.**, are related via the Equation (1):

$$h = h' \times \sin\beta / \sin(180 - \alpha - \beta) \quad (1)$$

where h is a real height of the point on a profile, h' is a height of the point on a registered profile, α is an angle between camera and surface, and β is an angle between laser and surface.

In most of the commercial laser profilometers used for materials testing, the *β* angle is equal to 90° (Mitaľ et al., 2019). The reason for that is a distortion of a profile line if that angle is less than 90° (Fig. 3). However, as seen in Equation 1, that reduces the vertical resolution of a profilometer. For the purpose of pavement surface analysis, the straightness of the profile is inconsequential because the pavement surface is usually irregular anyway, so the slope angle change in not as important, since the height difference is still accurate.

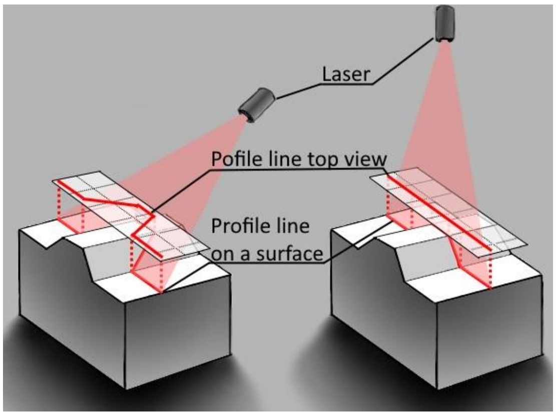

Figure 3. Distortion of a profile line

Lowering the angle increases the vertical resolution of a profilometer until the asperity slope and bottom cannot be reached by the camera and laser. In the case of a cone-shaped asperity (Fig. 4), the asperity wall and bottom can be seen on a profile only if both the camera (α) and laser (β) angles are greater than the angle of an asperity slope (γ). Overwise, the profile picture will contain discontinuities, which will add a significant error to the readings. Due to that reason, it is important to be able to change the angle to control the accuracy of the profilometer in a stage of profilometer verification.

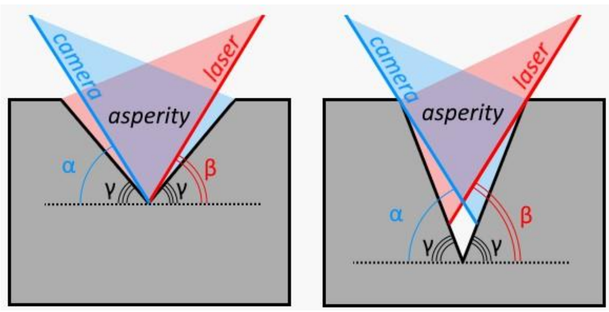

Figure 4. Distortion of a profile line

3.2 *Processing algorithm*

For this study, a data processing algorithm was also designed. It consisted of the following steps; profile registration, fine smothering, macrotexture filtration, texture parameter calculation.

The profile photo first needs to be processed to obtain a texture profile. First, pixel brightness is being calculated as well as the profile line brightness threshold. After that, points on a profile were calculated by finding the centre of brightness of each column of pixels. A registered profile then needs to be smothered to remove any errors. After that, a macrotexture filtration needs to be done. During that step, profile leveling was also obtained. Macrotexture filtration was not done during the verification of a profilometer since the data from the roughness tester was not filtrated. However, the same algorithm was used for profile leveling by increasing the approximation range. An example of a processed profile is shown in Figure 5. *S’* and *S* are fine smothering and filtration coefficients.

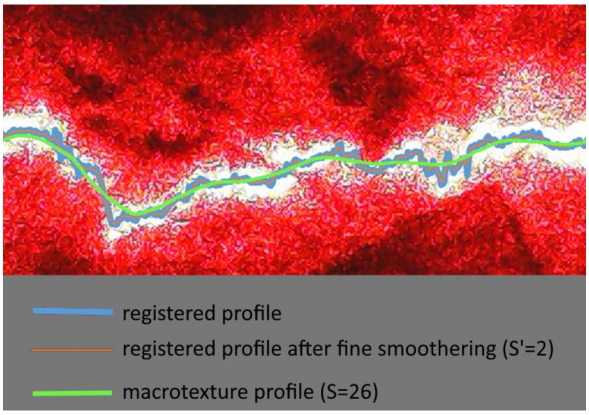

Figure 5. Processing of the photo of a profile (concrete texture)

For the fine smothering and filtration, an algorithm based on linear approximation, based on the method of least squares, was used. This algorithm approximates the line for each point based on the S-points before and after the point. Accordingly, the smothering coefficient is named *S'*, and the filtration coefficient is named *S*. The part of that line becomes the profile after smothering or a macrotexture profile line near the point. Microtexture was calculated as a distance between a point and the approximated line. The advantages of this linear approximation are simplicity and efficiency.

Conventional filtration algorithms, based on the Fourier transformation, the Butterworth filter, the Gaussian smoothing filter, or other frequency-based algorithms, calculate the microtexture as a height difference between a point and a macrotexture, which leads to an error (Edjeou et al., 2020). Algorithms based on the polynomial approximation can lead to "overfitting,” and they usually do not consider curved surfaces to be part of a microtexture, which is inappropriate for friction assessments because the overall grip is better on those surfaces. Plain surfaces, on the other hand, have the worst grip, and a polynomial approximation does not fit well to a straight line.

3.3 *Laser profilometer verification*

The laser profilometer verification was performed with different angles between the camera, laser, and a surface. The angle optimization was performed with the optimization of *S’* coefficient. The results of the optimization are presented in Table 1. In all sets of tests, the R^2 value between the roughness tester and laser profilometer results was calculated.

Table 1. Sets of tests for profilometer verification

Number of sets of tests	The angle between camera and surface (α), °	The angle between laser and surface (β), °	Theoretical vertical resolution of the profilometer, µm	Coefficient of determination between the roughness tester and profilometer (R^2)
1	45	45	4.31	0.92
2	45	90	8.61	0.95
3	60	90	12.18	0.89
4	60	60	6.09	0.99

As shown in Table 1, the optimal angle between the surface and both the laser and camera is equal to 60°. Although the lower angle increases the resolution of the profilometer, the profile discontinuities lower the total accuracy. Profile distortion with the change of an angle between laser and surface does not affect the accuracy that much compared to the reduction of vertical resolution.

As shown in Figure 6, where the results of the fourth set of tests are presented, the designed laser profilometer model's vertical resolution is much lower than the vertical resolution of the roughness tester, which leads to an error in the case of polished metal plates. However, proportionality of the results for polished metal plate was still obtained.

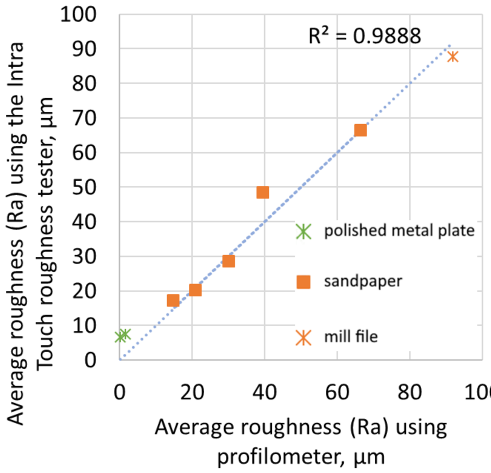

Figure 6. Profilometer verification results

4 CONCLUSION

The profile image assessment methodology presented in this paper can be used for the microtexture assessment. The smothering algorithm based on the linear approximation is simple and more suitable for friction assessment. Laser profilometry testing equipment for friction assessment can be cheap and reliable since friction assessment requires an analysis of texture wavelengths up to 0.5 mm. The laser profilometer model presented in this study is designed using cheap and common components and has a maximum vertical and horizontal resolution equal to 6 µm. Obtained results were verified with the stylus-based roughness tester; the R^2 coefficient is equal to 0.99.

5 REFERENCES

AAA. 2017. *Airport Practice Note 12 – Airfield Pavement Essentials.* Australia: Australian Airports Association.

Chen, S., Liu, X., Luo, H., Yu, J., Chen, F., Zhang, Y., Ma, T. & Huang, X. 2022. A state-of-the-art review of asphalt pavement surface texture and its measurement techniques. *Journal of Road Engineering*. 2(2):156–180. doi.org/10.1016/j.jreng.2022.05.003.

Dardano, J. & Wickham, G. 2005. *Australia's National Friction Testing Programme*. Available from: https://www.nzta.govt.nz/assets/resources/surface-friction-conference-2005/6/docs/australia-national-friction-testing-programme.pdf [Accessed 24 February 2022].

Edjeou, W., Cerezo, V., Zahouani, H. & Salvatore, F. 2020. Multiscale analyses of pavement texture during polishing. *Surface Topography: Metrology and Properties*. 8(2):024008. doi.org/10.1088/2051-672X/ab8f1b.

Li, Q.J., Zhan, Y., Yang, G. & Wang, K.C.P. 2020. Pavement skid resistance as a function of pavement surface and aggregate texture properties. *International Journal of Pavement Engineering*. 21(10):1159–1169. doi.org/10.1080/10298436.2018.1525489.

Martín-Béjar, S., Cañero-Nieto, J.M., Solano Martos, J.F. & Sevilla Hurtado, L. 2023. Laser Profilometry Application in Welding Geometrical Characterization. *Key Engineering Materials*. 960:65–72. doi.org/10.4028/p-2EHBlY.

Mitaľ, G., Dobránsky, J., Ružbarský, J. & Olejárová, Š. 2019. Application of Laser Profilometry to Evaluation of the Surface of the Workpiece Machined by Abrasive Waterjet Technology. *Applied Sciences*. 9(10):2134. doi.org/10.3390/app9102134.

Ueckermann, A., Wang, D., Oeser, M. & Steinauer, B. 2015. Calculation of skid resistance from texture measurements. *Journal of Traffic and Transportation Engineering (English Edition)*. 2(1):3–16. doi.org/10.1016/j.jtte.2015.01.001.

Wambold, J.C., Antie, C.E., Henry, J.J., Rado, Z., Descornet, G., Sandberg, U., Gothie, M. & Huschek, S. 1995. *International PIARC Experiment to Compare and Harmonize Texture and Skid Resistance Measurements*. Available from: https://www.piarc.org/ressources/publications/1/3832,01-04-T.PDF [Accessed 24 February 2022].

White, G. 2024. Comparison of bituminous surface options for regional airport runway pavements. In: *Bituminous Mixtures and Pavements VIII*. London: CRC Press. 355–363. doi.org/10.1201/9781003402541-42.

White, G., Ward, C. & Jamieson, S. 2021. Field evaluation of a handheld laser meter for pavement surface macro texture measurement. *International Journal of Pavement Engineering*. 22(8):950–959. doi.org/10.1080/10298436.2019.1654103.

Xiao, S., Xi, C., Xu, L., Li, J. & Tan, Y. 2024. Effects of road particulate contaminants on pavement skid resistance. *Road Materials and Pavement Design*. 25(4):874–887. doi.org/10.1080/14680629.2023.2229921.

Yang, G., Li, Q.J., Zhan, Y., Fei, Y. & Zhang, A. 2018. Convolutional Neural Network–Based Friction Model Using Pavement Texture Data. *Journal of Computing in Civil Engineering*. 32(6). doi.org/10.1061/(ASCE)CP.1943-5487.0000797.